Chapter 7

Thermal Properties of Porous Alumina Prepared using Rice Husk and Sucrose

7.1. Introduction

Thermal properties such as thermal conductivity and thermal shock resistance are key properties of porous ceramics for specific applications like burners, thermal barrier coatings, insulating refractories, heat exchangers, high temperature gas filters etc.[135-136] In such devices, thermal conductivity plays a major role in heat transfer calculations. Apart from these specific applications, effective thermal conductivity of ceramics is of general interest as it strongly influences other important properties such as thermal shock resistance and may exhibit certain features, in particular porosity dependence analogous to other properties e.g, electrical conductivity or elastic modulus.[137-141]

Similar to the other properties, e.g., strength, elastic modulus, electrical conductivity etc, thermal conductivity is also affected by the volume fraction of pores and pore microstructure (pore size, shape, connectivity, orientation etc). Thus, both porosity and pore microstructure play an important role in controlling effective thermal conductivity and ultimately the thermal shock resistance of porous ceramics. Depending on the application, either a high or a low thermal conductivity material is more desirable.[142] As per the requirement, thermal conductivity of ceramics can be very efficiently tailored by controlling the volume fraction of pores and pore microstructure of ceramics. To achieve a low thermal conductivity, the materials should contain a large volume fraction of pores, namely high porosity.

Though, Ugheoke et al. have studied the thermal insulating properties of kaolin-rice husk refractory bricks,[143] the results show limited microstructure and the dependence of thermal conductivity on porosity and pore size has not been reported.

The objective of this present study was to examine the influence of volume fraction porosity and pore size on thermal properties such as effective thermal conductivity and thermal shock resistance of the porous samples. Room temperature thermal conductivity was evaluated to investigate the effect of porosity, pore size

and pore connectivity on the measured thermal conductivity of porous alumina. Various analytical models were used to predict the effective thermal conductivity of the porous alumina for comparison of experimental values obtained in the present work.

7.2. Sample Preparation and Characterization

Sample preparation was same as already mentioned in chapter 5, except that the sample size for measurement of thermal conductivity. Room temperature thermal conductivity of porous alumina samples was measured using a hot disk thermal analyzer (TPS 2500s, Hot disk AB Co. Sweden adopting the TPS technique). The hot disk sensor consists of an electrically conducting pattern in the shape of a double spiral which is laminated between two thin sheets of insulating material (kapton). The hot disk sensor was sandwiched between two identical pieces of alumina samples during measurement. The transient techniques on the other hand, measure a response as a signal is sent to create heat in the sample. Therefore, these techniques are distinguished mainly by the short time required to obtain the desired results. One of the main advantages of transient techniques over steady state techniques is that the influence of the contact resistance can be removed in the analysis of experimental data. This enables accurate measurements over a wide range of thermal conductivity and therefore a wide range of different materials.

7.3. Theory

7.3.1. Thermal conductivity

Heat transfer in porous ceramics is a complicated process which generally occurs by three mechanisms: conduction, convection, and radiation. However, in many cases the latter two are usually smaller than the conduction and hence can be neglected. Convection hear transfer takes place with the condition that Grashof number defined as

$$G_r = \frac{\left(g\beta \, \Delta T \, D^3 \rho^3 \right)}{\eta^2} \quad \text{.....(7.1)}$$

exceeds a value of 1000, where g= 9.81 m/s^2 is the gravitational acceleration, β the volumetric thermal expansion co-efficient of the pore gas (considered to be an ideal gas, i.e., β= 1/v, with v being the absolute Kelvin temperature), ΔT the temperature difference across one pore, D the pore size (diameter), ρ and η the density and viscosity of the gas respectively.[2] Applying plausible estimates for the variables, considering air at room temperature and at 1 atmospheric pressure (density, ρ= 1 kg/m^3, and viscosity, η= 2x10^{-5} Pa.s) the critical pore size is L_{crit}= 10 mm for a temperature difference of 10˚C. Another condition for convection to take place, is that the pores must be open and interconnected. In the present study the pore size considered is much smaller than 10 mm and thus convection mechanism can be ignored.

Radiation heat transfer can be expressed using Stefan-Boltzmann radiation law.[144] Radiation effect is negligible compared to conduction when the dimensionless ratio denoted as

$$\frac{\left(4\gamma\sigma\ \varepsilon\ DT^3\right)}{k_o} \quad \text{.....(7.2)}$$

is much smaller than unity (<< 1). In this ratio, γ is a geometric factor of the order of unity (.45 for spherical pores), ε is the emissivity of the pore surface (0.38$\pm$0.10 for alumina), σ is the Stefan-Boltzmann radiation constant (5.67x10^{-8} W/m^2 K^4) D is the pore size, T is the average Kelvin temperature and k_0 is the conductivity of the solid phase.[145] Inserting these values one obtains at RT a radiation contribution of 7.26x10^{-3} W/mK which is clearly negligible with respect to the thermal conductivity of the solid phase (dense alumina) which is approximately 35 W/mK at RT.[146] When heat transfer through convection and radiation is negligible, the effective heat transfer is the contribution from conduction mechanism.

In heterogeneous materials, the presence of pores yields local changes in the thermal conductivity. At macroscopic scale of sample dimensions, the measured value of thermal conductivity can be defined as that of an equivalent homogeneous medium, denoted strictly as the equivalent thermal conductivity. There are various models which describe the equivalent thermal conductivity of porous crystalline

ceramics. Since porous materials can be considered as a special case of composite (pore phase dispersed in alumina matrix phase), the equivalent thermal conductivity of porous materials depends on the volume fraction of pores, their shape and connectivity, their orientation and at higher temperature the emissivity of the pore-solid interface. A wide range of models have been proposed in the literature to take these various –situations into account.[147-148] Many effective thermal conductivity models found in the literature are based on one or more of the five basic structural models: specifically, the series, parallel, Maxwell-Eucken (two forms)[149-150] and Effective Medium theory (EMT) models.[151-152] The physical structures assumed in the derivations of the series and parallel models are of layers of the components aligned either perpendicular or parallel to the heat flow as their names indicate. The Maxwell-Eucken model assumes a dispersion of small spheres within a continuous matrix of a different component with spheres being far enough apart such that the local distortions in the temperature distributions around each of the spheres do not interfere with their neighbor's temperature distribution. For a two-component material, two forms of the Maxwell-Eucken model arise depending on which of the components form the continuous phase. Maxwell-Eucken equation is for materials containging up to ~10% dispersed phase.[144] With higher pore content, non spherical shape of pores can not be ignored. An appropriate model is given by the effective medium theory (EMT) which predicts the equivalent conductivity of a mixture with random distribution of two components with different conductivities. The EMT model assumes a completely random distribution of phases with pore volume fraction being higher than 0.15.[144]

For EMT theory to be applicable for porous materials, the characteristic parameters such as relative amount of different phases, volume fraction porosity, shape, orientation, and distribution of pores are equally important.[153] If for instance, the pores are shaped as thin lamellae oriented perpendicular to heat flow, they would have a far stronger effect on the thermal conductivity than if they were spherical. Similar to the connectivity of phases in a composite material, the connectivity of the pore phase is also a key feature of porous materials. In analogous to a composite consisting of polymer filled with ellipsoid metal particles

which may have a 3-0, 3-3 or 0-3 connectivity depending on whether or not the metal particles build a conductive network.[154] As per the above theory, the RH based porous ceramics developed in our case can be categorized as alumina matrix with either isolated pores, 3-0 type or inter connected pores, 3-3 type. The first number (3) indicates that the ceramic particles are self-connected in all three directions because it is the matrix. The second number (3 or 0) indicates in how many directions the pores are self-connected. The 3-0 type sample is equivalent to unconnected/isolated pores in a continuous ceramic matrix whereas the 3-3 type sample has interconnected networks of both solid ceramic and pores. The 0-3 connectivity is strictly not possible in our case, as the ceramic grains are being inter connected only at a few tiny points which would fall apart and thus lowers the strength of porous compacts.

A common effective medium theory describing the thermal conductivity and other physical properties of such type of microstructure was introduced by Garnet. Accordingly, the thermal conductivity of a mixture of unconnected /isolated pores with thermal conductivity k_d dispersed in a ceramic matrix (alumina in this case) with thermal conductivity k_m is given as

$$k_c = k_m \frac{Lk_d + (1-L)k_m + f(1-L)(k_d - k_m)}{Lk_d + (1-L)k_m - fL(k_d - k_m)} \quad \text{.....(7.3)}$$

where f is the volume fraction of dispersed pore phase. Eqn. 7.3 is the general form of Maxwell theory with oriented ellipsoidal dispersed phase. L is the depolarization factor of the ellipsoids in the direction of heat flow: L= 1/3 (or 0.33) for spherical second phase; 1/3 > L> 0 (or 0-0.33) for prolate ellipsoids; 1> L > 1/3 (or 0.33-1) for oblate ellipsoids. If the dispersed phase has poor conductivity and f is small, then the Maxwell-Garnet equation can be written as

$$k_c = k_m \left(1 - \frac{f}{1-L}\right) \quad \text{.....(7.4)}$$

This Eqn. 7.4 is only valid for samples with 3-0 type microstructure. For samples with 3-3 type connectivity, the Bruggeman symmetric effective medium

theory is more suitable.[155] The thermal conductivity can be calculated from the Eqn. 7.5.

$$f\frac{k_1-k_c}{k_c+L_1(k_1-k_c)}+(1-f)\frac{k_2-k_c}{k_c+L(k_2-k_c)}=0.....(7.5)$$

where k_d, k_m and k_c are the thermal conductivities of dispersed phase, matrix phase and the porous composite respectively. The volume fraction of dispersed phase being f and the depolarization factors of ellipsoids of dispersed phase and matrix phase being L_d and L_m respectively. Considering, $L_d = L_m = L$ and K_d is negligible in comparison to K_m, the simplified equation can be expressed as

$$k_c = k_m\left[\frac{(L-1)(1-f)}{f}+L\right].....(7.6)$$

7.3.2. Thermal shock resistance

When a solid is exposed to a sudden change of surface temperature, thermal stresses appear within it which if sufficiently large can cause cracking and spalling; that is, loss of material from the surface as flakes or chips. Generally speaking, thermal stresses are to be avoided, since they significantly weaken a component. In extreme cases, a part can spontaneously crumble during cooling. Rapid heating or cooling of a ceramic will often result in its failure. This kind of failure is known as thermal shock and occurs when thermal gradients and corresponding thermal stresses exceed the strength of the part. For instance, when a component is rapidly cooled from a temperature T to T_0 , the surface will tend to contract but will be prevented from doing so by the bulk of the component that is still at temperature T. In such a situation surface tensile stresses would be generated that have to be counter balanced by compressive ones in the bulk.

Thermal shock resistance is usually evaluated by heating samples to various temperatures T_{max}. The samples are rapidly cooled by quenching them from T_{max} into a medium, most commonly ambient temperature water. The post quench retained strengths are measured and plotted versus the severity of the quench, or $\Delta T = T_{max}-T_{ambi}$. The salient feature of the experiment is that the occurrence of a rapid decrease in retained strength around a critical temperature difference ΔT_c below

which the original strength is retained. As the quench temperature is further increased, the strength decreases but more gradually. From a practical point of view, it is important to be able to predict ΔT_c. By understanding the various parameters that affect thermal shock, successful design of solids which are resistant to thermal shock can be made.

Physics of events occurring during thermal shock, subjecting a solid to a rapid change in temperature results in differential dimensional changes in various parts of the body and build up stresses within it. Consequently the strain energy of the system will increase. If the strain energy increase is not too large, i.e., for small ΔT values, the preexisting cracks will not grow and the solid will not be affected by the thermal shock. However, if the thermal shock is large, the many cracks present in the solid will extend and absorb that excess strain energy. Since the available strain energy is finite, the cracks will extend only until most of the strain energy is converted in to surface energy at which point they will be arrested. The final length to which the cracks will grow will depend on their initial size and density. If only a few, small cracks are present, then their final length will be quite large and the degradation in strength will be high. Conversely, if there are numerous small cracks, then each will extend by a small amount and the corresponding degradation in strength will not be that severe. In latter case, the solid is considered to be thermal-shock-tolerant.

Now, it is necessary to highlight the important parameters that render a ceramic resistant to thermal shock. If a block of the solid, initially at an uniform temperature T_1 is suddenly cooled (by dropping into ice/water), its surface temperature will drop to T_2, contracting the surface layers of the block and producing a thermal strain of $\alpha\ \Delta T$, where α is the thermal expansion co-efficient and ΔT is the difference between T_1 and T_2. But the surface is strongly bonded to the underlying mass of the block constraining it to its original dimensions and producing a thermal stress of

$$\sigma_f = \frac{E\alpha\Delta T}{(1-\upsilon)} \qquad \text{.....(7.7)}$$

in the surface. When this stress exceeds the fracture strength of the material, σ_f , it cracks and spalls. The thermal shock resistance is measured by the temperature drop which will just cause cracking.

$$\Delta T_c = \frac{\sigma_f (1-\upsilon)}{(E\alpha)} \quad \text{.....(7.8)}$$

The modulus of a cellular solid is approximately

$$E^* = Es\left(\frac{\rho^*}{\rho_s}\right)^2 \quad \text{.....(7.9)}$$

The fracture strength (is equal to crushing strength) is

$$\sigma_f^* = .65\left(\frac{\rho^*}{\rho_s}\right)^{3/2} x\sigma_{fs} \quad \text{.....(7.10)}$$

and the thermal expansion,

$$\Delta T_c = 0.65\ \Delta T_{cs}\left(\frac{\rho^*}{\rho_s}\right)^{1/2} \quad \text{.....(7.11)}$$

where $\Delta T_{cs} = \sigma_{fs} / E_s\alpha_s$ is the thermal shock resistance of the fully dense solid.

In general, the thermal shock resistance increases as the density of the porous solid decreases. This is because the network of struts which make up a low density porous solid can accommodate the thermal strain by bending.[156] This property of porous solids is exploited in low density refractories.

7.4. Results and Discussion

7.4.1. Thermal conductivity

A. Experimental results

The thermal conductivity measurements carried out by TPS technique at room temperature in the present study has been mentioned in the experimental procedure. The main advantages of the hot disk technique include wide thermal conductivity range (0.005-500 W/mK), wide range of material types, easy sample preparation, nondestructive measurement and high accuracy. The results of porosity

and pore size dependence of thermal conductivity measurements are summarized in Fig. 7.1 and Fig. 7.2.

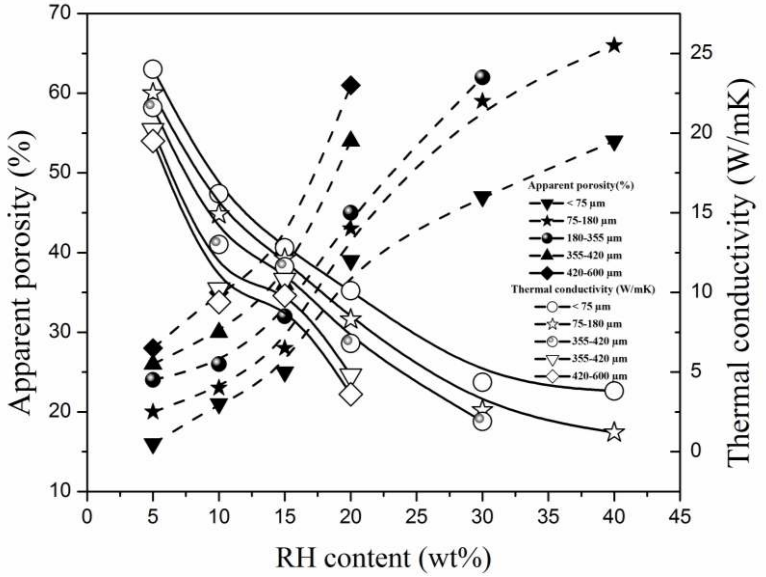

Fig. 7.1 Effect of RH content and RH size on porosity and thermal conductivity of porous alumina compacts.

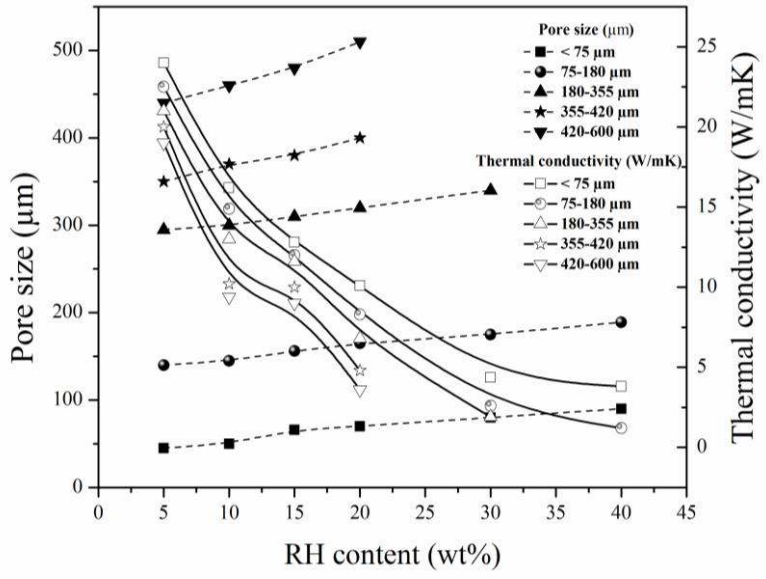

Fig. 7.2 Variation of RH size and RH content on pore size and thermal conductivity of porous alumina compacts

The thermal conductivity decreases significantly with increasing volume fraction of porosity. Also, the conductivity increases with particle size of RH pore

former. This suggests that porosity and pore size are very effective parameters for tailoring thermal conductivity. The thermal conductivity of porous alumina decreases from 24 W/mK to 1.2 W/mK with increase in volume fraction porosity from 20 to 66% and pore size from 50 to 516 µm.

Effect of volume fraction RH and size of RH powder in the composition, on room temperature thermal conductivity of corresponding sintered porous alumina samples has been shown in Table 7.1 &7.2.

Table 7.1 Experimental and predicted (EMT) thermal conductivity of porous alumina compacts fabricated using (a) 10, (b) 20, (c) 30 and (d) 40 wt% RH (75-180) µm average Size.

Composition		Overall porosity (vol %)	Avg. pore size (µm)	Pore Microstructure (Interconnected/Isolated)	Experimental Thermal conductivity (W/mK)	Relative thermal conductivity	Thermal conductivity (EMT) (W/mK)
RH size	RH (wt%)						
75-180 µm	(a) 10	24	145	Isolated + interconnected	21.62	0.27	22.27
	(b) 20	45	155	interconnected	8.3	0.12	7.63
	(c)30	62	160	interconnected	2.6	0.02	0.88
	(d) 40	66	165	interconnected	1.2	0.005	0.02

Typical values of relative thermal conductivity for samples with compositions Al_$^{75\text{-}180}$RH$_{10}$_SS$_{20}$, Al_$^{75\text{-}180}$RH$_{20}$_SS$_{20}$, Al_$^{75\text{-}180}$RH$_{30}$_SS$_{20}$, Al_$^{75\text{-}180}$ RH$_{40}$_SS$_{20}$, having porosity values 24%, 45%, 62% and 66%, pore size 145 µm, 155 µm, 158 µm, 160 µm are 0.27, 0.12, .02 and 0.005 respectively (Table 7.1). Similarly, the relative thermal conductivity values for samples with compositions Al_$^{<75}$RH$_{20}$_SS$_{20}$, Al_$^{75\text{-}180}$RH$_{20}$_SS$_{20}$, Al_$^{75\text{-}180}$ RH$_{20}$_SS$_{20}$, Al_$^{355\text{-}420}$RH$_{20}$_SS$_{20}$, having porosities 39%, 45%, 50% , 54% and 61% , and pore sizes 55 µm, 155 µm, 310 µm, 375 µm and 530 µm are 0.125, 0.12, 0.107, 0.048 and 0.012 respectively (Table 7.2)

Table 7.2 Experimental and predicted (EMT) thermal conductivity of porous alumina compacts fabricated using 20 wt% RH powder with (a) < 75 (b) 75-180 (c) 180-355 (d) 355-420 and (e) 420-600 µm size.

Composition		Overall porosity (vol%)	Avg. pore size (µm)	Pore Microstructure (Interconnected/ Isolated)	Experimental Thermal conductivity (W/mK)	Relative thermal conductivity	Thermal conductivity (W/mK)
RH Content (wt%)	RH size (µm)						
20	(a) < 75	39	64	interconnected	10.1	0.125	12.09
	(b) 75-180	45	155	interconnected	8.3	0.12	7.63
	(c)180-355	50	310	interconnected	6.8	.107	6.36
	(d) 355-420	54	370	interconnected	4.8	0.048	5.09
	(e) 420-600	61	525	interconnected	3.6	0.012	1.55

Pabst et al. reported porous alumina with relative thermal conductivity 0.2-0.9 for a sample porosity of 10-50 %, prepared using starch as pore forming agent.[141] Similarly, Gregorova et al. reported relative thermal conductivity of porous alumina in the range 0.14-0.85 for a porosity of 10-42 %, prepared by slip casting.[157] Our experimental thermal conductivity values are comparatively lower in comparison to the reported values, as given above, for the similar porosity range. This may be due to the difference in pore morphology and extent of interconnection in porous alumina fabricated using rice husk and though other processes.

In a recent review of the influence of the porosity on physical properties, Rice et al.[134] reported significance of percolation limit, P_c (critical porosity limit), which is a value of P (volume fraction porosity) above which a specific physical property (e.g, thermal conductivity, elastic modulus etc.) is insensitive to further changes in porosity or relative density At $P > P_c$, the particle–particle contact is insufficient to fully transmit the physical forces. Following Rice we calculate that $P_c = 0.5$. This number corresponds to an average relative density of 50% which is near the average relative density of a green body powder compact. Thus, it implies that the low thermal conductivity results primarily from the low solid area fraction

(SAF) available for heat flow. Thus, it can be inferred that material linkage dominates room temperature heat flow in porous materials. Similar to the percolation limit for porosity, the corresponding limit for pore size is approximately 400 μm beyond which the properties are almost independent of the pore size. Thus, it is suggested that the heat flow is controlled by the particle-particle cross-sectional contact area which is dependent on the porosity and pore microstructure.

B. Comparison of experimental results with predicted results

The porous alumina ceramics fabricated in this process can be considered as a two phase system, viz. a dense solid alumina skeleton as matrix phase and air (pore) as dispersed phase. The microstructure of the obtained porous samples can be represented as one of the schematic diagrams given in Fig. 7.3 (a)-(c). The schematic diagram in Fig. 7.3 (a), which represents sample microstructure with isolated pores is similar to (3, 0) model of EMT theory. The schematic in Fig. (b) and Fig. (c), representing sample microstructure with interconnected pores with varying extent of interconnection, are equivalent to (3, 3) model in EMT theory.

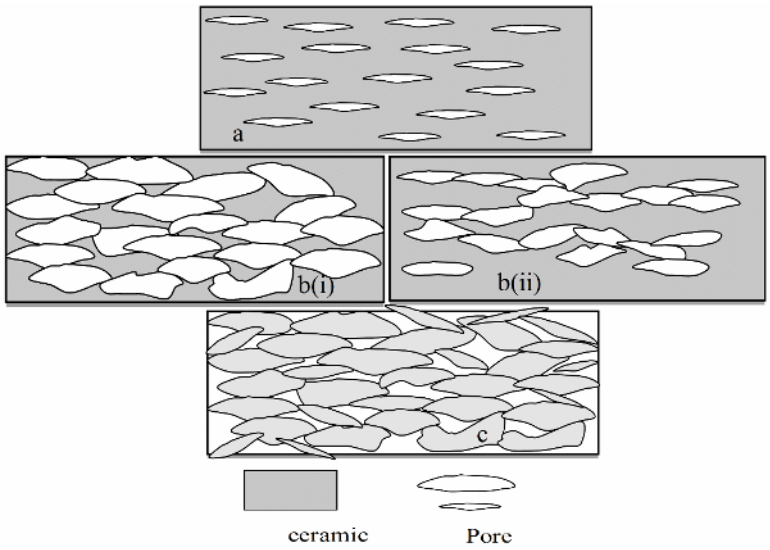

Fig. 7.3 Schematic representation of three different types of pore connectivity for developed porous ceramics (a) 3-0 connectivity (b) (i) and (ii) 3-3 connectivity with varying extent of interconnection & (c) 0-3 connectivity

In Fig. 7.4, it can be found that the experimental data are in close agreement with the EMT equation. The result is attributed to the effective thermal conductivity for a two phase system depending on the porosity of porous alumina samples. It is interesting to note that the effective thermal conductivity of samples with fully isolated pores and those with fully interconnected pores is overlapping with the predicted values. In contrast, thermal conductivity of samples with partially interconnected pore microstructure (many interconnected pores and a few isolated pores) are not ideally fitted to the prediction curve. This may be due to the reason that the fine pores created due to sucrose burn out have not been considered for calculation of the effective thermal conductivity.

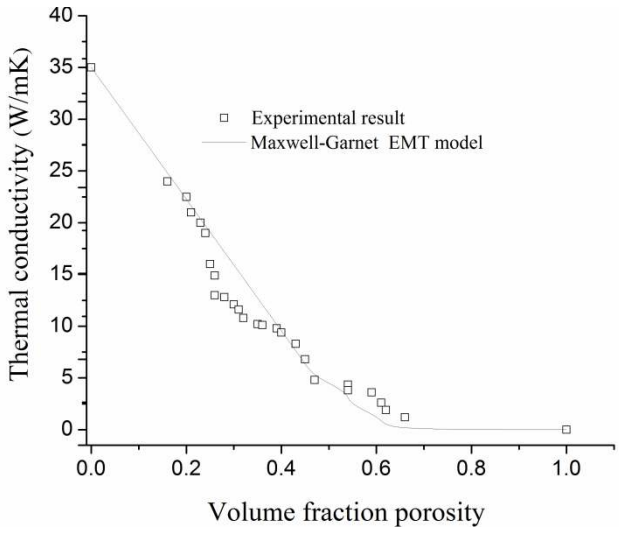

Fig. 7.4 Effective thermal conductivity as a function of porosity for analytical prediction and experimental measurements

The prediction of the dependence of the effective thermal conductivity with porosity and pore size by analytical calculations requires knowledge of the thermal conductivity of each phase. The thermal conductivity of air and dense alumina were chosen to be 0.026 and 35 W/mK from literature values.[134] Fig. 7.4 shows the influence of porosity on thermal conductivity of porous alumina ceramics compared with the predicted values based on EMT equation for the ellipsoidal dispersed phase of (3,0) and (3,3) type, as has already been mentioned in theory section. In this plot, it is assumed that there is 3-0 connectivity in the sample microstructure for isolated pores and 3-3 connectivity for the samples with interconnected microstructure.

Similarly, the effect of pore size on effective thermal conductivity of samples along with the predicted values has been displayed in Fig. 7.5. The experimental data are in close agreement with the predicted values for most of the samples (with fully isolated and fully interconnected pore microstructure), except a few samples which possess a mixture of isolated and interconnected pores (partially interconnected microstructure). The observed behavior is similar to that represented in Fig. 7.5. Minor deviation in the thermal conductivity values can be linked to samples with partially interconnected microstructure (intermediate type of microstructure in between (3, 0) and (3.3) type).

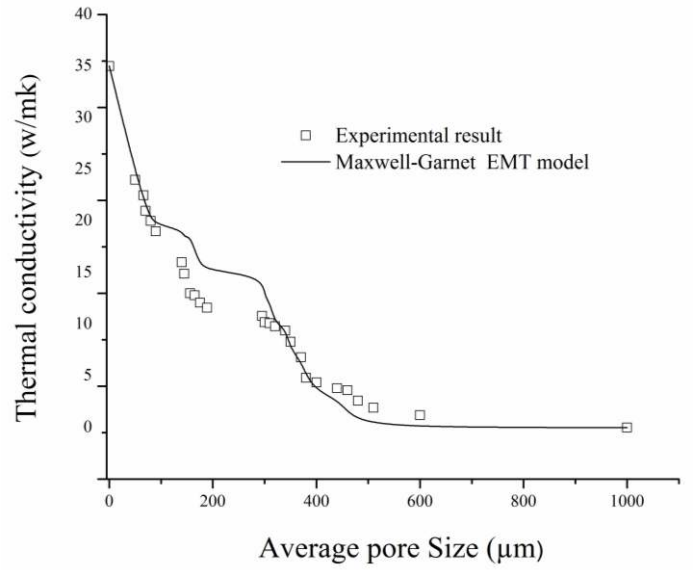

Fig. 7.5 Effective thermal conductivity as a function of pore size for analytical prediction and experimental measurements

Thus, the thermal conductivity of porous ceramics with tailored microstructure fabricated in the present process is well fitted to the EMT model. Fig. 7.4 and Fig. 7.5 show a best fit of the Maxwell-Garnet and Maxwell-Bruggeman theory for the thermal conductivity of porous alumina samples having isolated and/or interconnected porous microstructure respectively. The idea of comparison was to investigate how well the theoretical models fit to the experimental data and from that draw some conclusion about the microstructure of porous ceramics.

7.4.2. Thermal shock resistance

The retained strengths of the porous alumina ceramics having different porosities after thermal shocking at different ice quenching temperatures (ΔT) are shown in Fig. 7.6. Roughly the flexural strength of porous alumina decreases with increasing the thermal shock temperature difference at any given porosity of sample.

According to the nature of the curves, it can be classified into two groups: first, the abrupt decrease in retained flexural strength (Fig. 7.6 (a)-(c)) for porous alumina samples having porosity up to 45% and second, the gradual decrease of retained strength as the sample was tested above a critical quenching temperature (Fig. 7.6 (d and e) for samples with porosity greater than 45%. Meanwhile, the residual strength of the samples also exhibits a more complex evolution with increasing the quenching temperature difference from 0 to 800˚C (Fig. 7.6 (a)-(c)) i.e., moderate degradation→rapid degradation→moderate degradation. The critical temperature difference lies somewhere in the temperature range between 200-600˚C. A series of quenching experiments in the intermediate temperatures can give a better clarity regarding a single (more) exact ΔT_cvalue. It can be seen that the presence of a broad range (200-600˚C) of critical temperature difference exists for samples with lesser porosity whereas for samples having porosities 54% and 61%, critical ΔTc range was almost absent. In comparison, the ΔT_c value for single crystal alumina and dense polycrystalline alumina with grain size 10 μm is within 200-300˚C.[158] This confirms that the presence of pores broadened the value of ΔT_c in porous alumina.

It is well known that pores in the specimens would effectively relax the thermal shock stress and arrest the propagation of pre-existing microcracks. For specimens with less porosity, the thermal shock stress can not be completely relaxed by the pores so that new cracks can be produced for the sake of absorbing the extra thermal shock energy resulting in higher strength degradation. If the porosity is high (>22% in the present case), a crack may be arrested or deflected when it reaches a pore. The pore consumes some of the thermal shock stress .[156] As a consequence, the crack propagation becomes much more difficult in presence of

pores in porous ceramics. The residual strength was higher for samples having less porosity and vice versa for sample with more porosity.

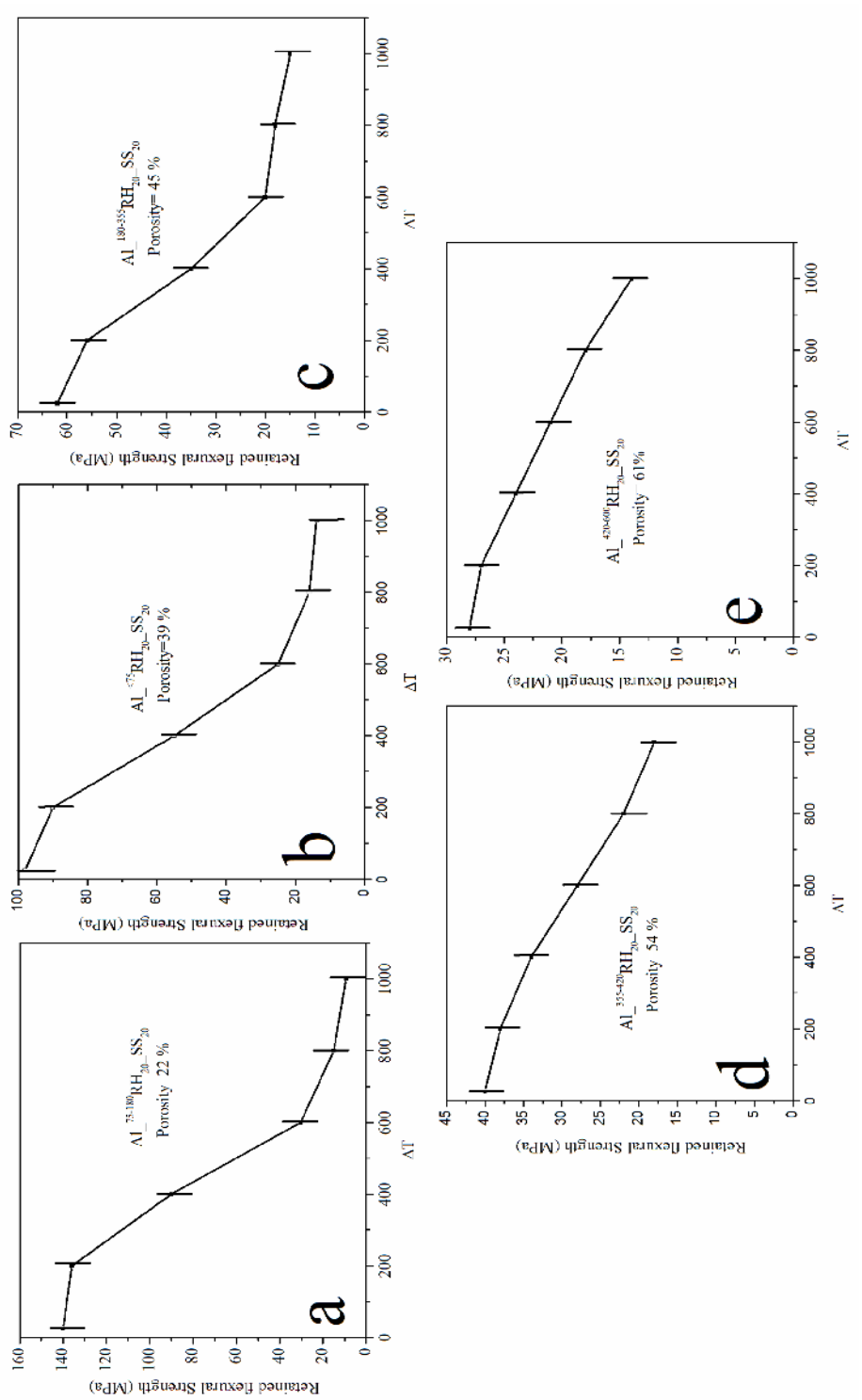

Fig. 7.6 Retained flexural strength as a function of severity of quench (temperature difference in quenching) for porous alumina with varying porosity

Fig. 7.7 shows strength of samples after two cycle of quenching for samples with 10 and 20 wt% RH. It is interesting to note that though decrease in magnitude of strength is more than half of the initial strength after two cycles, samples did not show any surface crack or deterioration followed by quenching. A series of quenching cycles performed for a sample with composition Al_$^{420\text{-}600}$RH$_{20}$_SS$_{20}$ resulted in cracking and disintegration of the sample after 20th cycle. Thus, it is clear from the above observation that though decrease in strength is rapid during initial thermal cycles, degradation is slow during subsequent cycles. A comparison with quenching of a dense alumina sample shows that dense sample failed after 5th cycle.

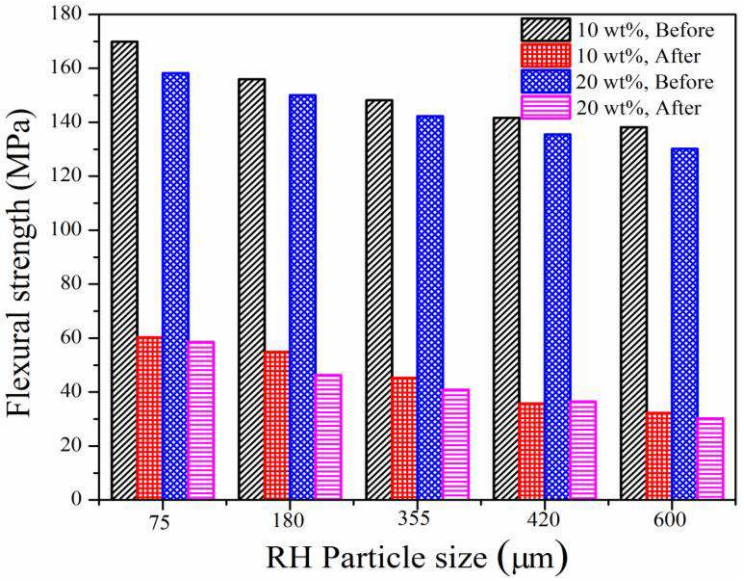

Fig. 7.7 Effect of composition on flexural strength before and after thermal quenching

Higher thermal shock resistance of the of the developed porous alumina can be attributed to two factors such as (a) presence of pores and (ii) formation of minor mullite phase due to addition of RH. The combined effect of above two factors contributed to excellent thermal shock resistance. The presence of pore boundaries accommodates the thermal strain through bending, and thus resists the propagation of crack.[156]

7.5. Summary

1. Thermal conductivity of the developed samples was characterized by the TPS technique at room temperature. From the view point of heat conduction, the porous samples can be considered as a two phase system, viz. a dense alumina skeleton and air, and the thermal conductivity can be used to describe heat transfer through this two-phase system.

2. The thermal conductivity of the developed samples was in the range 1.2. to 24 W/mK.

3. The experimental results were compared to the chosen analytical model, effective medium theory (EMT) for ellipsoidal shape dispersed phase in a continuous matrix. The sample microstructures were categorized in to (3, 0) type for isolated pore phase (Maxwell-Garnet equation) and (3, 3) type for interconnected pore phase (Bruggner equation).

4. The experimental results are shown to agree closely with the predictions made by the above two models of the EMT theory for two phase system. Little deviation from the predicted values of thermal conductivity for few samples in the intermediate range of porosity and pore size can be attributed to the partially interconnected microstructure, which do not exactly fit in to either (3,0) type or (3,3) type.

5. The nature of the thermal shock resistance curve related to decrease in strength for samples with porosity up to 45% (1st case) was different from that observed for samples having porosity above 45%.

6. In the 1st case (Fig. 7.6 (a)-(c)), the retained strength was initially moderate followed by a rapid decreasing trend in the intermediate range. Then finally a gain a moderate decrease in retained strength was observed. The critical quenching temperature (ΔT_c) of porous alumina was approximately in the range 200-600˚C for samples having porosity lesser than equal to 45%.

7. Samples with much higher porosity (P > 45%), the decrease in retained strength was much gradual and no ΔT_c value was seen.

8. A typical sample Al_$^{420\text{-}600}$RH$_{20}$_SS$_{20}$ could withstand the severity of quenching up to 20 cycles, where as in comparison, a dense alumina failed after 5th cycle.